Original Article

Targeted deep sequencing reveals the genetic heterogeneity in well-differentiated pancreatic neuroendocrine tumors with liver metastasis

Wentao Zhou[1], Xu Han[1], Yuan Ji[2], Dansong Wang[1], Dong Xie[3], Zilong Qiu[4], Wenhui Lou[1,5]

[1]Department of Pancreatic Surgery, Zhongshan Hospital, Fudan University, Shanghai, China; [2]Department of Pathology, Zhongshan Hospital, Fudan University, Shanghai, China; [3]CAS Key Laboratory of Nutrition, Metabolism and Food Safety, Shanghai Institute of Nutrition and Health, University of Chinese Academy of Sciences, Chinese Academy of Sciences, Shanghai, China; [4]Institute of Neuroscience, State Key Laboratory of Neuroscience, Chinese Academy of Sciences Center for Excellence in Brain Science and Intelligence Technology, Chinese Academy of Sciences, Shanghai, China; [5]Department of General Surgery, Qingpu Branch of Zhongshan Hospital Affiliated to Fudan University, Shanghai, China

Contributions: (I) Conception and design: W Lou, Z Qiu, D Xie; (II) Administrative support: W Lou, Z Qiu; (III) Provision of study materials or patients: Y Ji, D Wang, D Xie; (IV) Collection and assembly of data: W Zhou, Y Ji, D Wang; (V) Data analysis and interpretation: W Zhou, X Han, Y Ji, D Wang; (VI) Manuscript writing: All authors; (VII) Final approval of manuscript: All authors.

Correspondence to: Wenhui Lou. Department of Pancreatic Surgery, Zhongshan Hospital, Fudan University, 180 Fenglin Road, Xuhui District, Shanghai 200032, China. Email: lou.wenhui@outlook.com; Zilong Qiu. Institute of Neuroscience, State Key Laboratory of Neuroscience, Chinese Academy of Sciences Center for Excellence in Brain Science and Intelligence Technology, Chinese Academy of Sciences, 320 Yueyang Road, Xuhui District, Shanghai 200031, China. Email: zqiu@ion.ac.cn.

Background: Pancreatic neuroendocrine tumor is a rare and heterogeneous entity, and approximately half of the patients harbored liver metastasis when initially diagnosed, whose prognosis is dismal. High-throughput sequencing has largely uncovered the genomic features of pancreatic neuroendocrine tumor, but the genetic alterations in the metastatic cases remain relatively unclear, which we aimed to study.

Methods: Pathologically confirmed well-differentiated pancreatic neuroendocrine tumor samples resected in our hospital from 2000 to 2019 were collected. We performed deep sequencing on the exome of 341 tumor-related genes, and compared the differences of genetic alterations between the metastatic and the non-metastatic cases, as well as between the primary and the paired liver metastatic tumors.

Results: Sequencing data of 79 samples from 29 pancreatic neuroendocrine tumor patients were included into analysis. A total of 2,471 somatic variants were identified, 75.5% of which were considered as low-abundance. *NOTCH1* was the most frequently mutated gene, altered in 26 (53.1%) pancreatic neuroendocrine tumor samples from 18 (62.1%) patients. Compared with the non-metastatic pancreatic neuroendocrine tumors, the metastatic cases were discovered with more single nucleotide variants and copy number variations, indicating the increased genomic instability. In addition, among the paired metastatic cases, the primary and the metastatic lesions shared limited mutated genes.

Conclusions: Through the targeted deep sequencing, we identified the intratumor, intraindividual, and interindividual heterogeneity in the pancreatic neuroendocrine tumor patients, particularly in the metastatic cases, bringing potential challenges for the current biopsy strategies in guiding clinical treatments.

Keywords: Pancreatic neuroendocrine tumor (pNET); liver metastasis; targeted sequencing; genomic alteration; heterogeneity

Submitted Oct 03, 2021. Accepted for publication Feb 10, 2022. Published online May 19, 2022.
doi: 10.21037/hbsn-21-413
View this article at: https://dx.doi.org/10.21037/hbsn-21-413

Introduction

Pancreatic neuroendocrine tumor (pNET) is a relatively rare entity originating from the pancreatic islets, and accounts for 2–5% of all pancreatic malignancies (1,2). Featured with heterogeneity, pNETs display variable histological characteristics and clinical courses. The large proportion of pNETs appear in an indolent manner compared with the ductal adenocarcinoma, which could obtain an oncological cure after the radical resection. On the contrary, the rest parts progress aggressively, presenting with synchronous distant metastasis or short-term postoperative recurrence. Liver is the most common metastatic site, which is mainly ascribed to the anatomical return of pancreatic veins, and the metastatic pNET patients suffer from a dismal prognosis with median survival less than three years (3,4). Currently, the metastatic mechanism of pNET remains largely unknown.

Benefitting from the high-throughput sequencing technique, the genetic alterations of pNET have been gradually revealed. Jiao *et al.* (5) reported the frequently mutated genes involving chromatin remodeling (*MEN1*, *ATRX* and *DAXX*) and mTOR pathway by the whole-exome sequencing of pNET. Consistent with these discoveries, Scarpa *et al.* (6) also uncovered the important *MUTYH* inactivation and potential novel activation mechanisms of mTOR pathway, including *DEPDC5* mutation, *EWSR1* fusion and *PSPN* amplification, with the largest whole-genome sequencing cohort. In contrast to primary pNET, Roy *et al.* (7) showed the different characteristics of metastatic pNET that 75% of the lesions harbored *CDKN2A* copy number loss and 50% harbored chromatin remodeling gene (*SETD2*, *ARID1A*, *CHD8* and *DNMT1*) alterations. Recently, Pea *et al.* (8) described the features of small pNET with high liver metastatic risks as frequent alterations in driver genes and recurrent chromosomal gains and copy neutral loss of heterozygosity (CN-LOH) through targeted sequencing and single nucleotide polymorphism array. However, the genetic landscapes of liver metastatic pNET were still unclear due to its diversity as well as the distinct sequencing strategies.

Herein, we performed targeted sequencing with a custom panel of 341 genes, the majority of which have been proven as driver genes in various tumors. We aimed to deepen the understanding about the genomic differences between the metastatic and the non-metastatic pNETs, as well as between the primary and the paired liver metastatic tumors. We present this article in accordance with the STREGA reporting checklist (available at https://hbsn.amegroups.com/article/view/10.21037/hbsn-21-413/rc).

Methods

Patients and clinical samples

Patients who underwent surgical resection for well-differentiated pNET with liver metastasis in Zhongshan Hospital, Fudan University from January 2000 to December 2017 were carefully reviewed. Formalin-fixed, paraffin-embedded (FFPE) samples of liver metastasis, paired primary tumor (if available) and adjacent normal tissue were collected. The tumor and normal areas of FFPE samples were marked after the corresponding hematoxylin and eosin-stained sections were reviewed by an experienced pathologist. Then, 5 mm-sized cores were punched from the marked areas for DNA extraction. Fresh tumor tissues and peripheral blood samples were collected from the consecutive well-differentiated pNET patients who underwent surgery in our hospital from January 2018 to March 2019. FFPE samples from 16 cases and fresh samples from 14 cases were performed with sequencing, and case five was excluded since the phylogenetic analysis showed that the samples from this patient were unmatched (Figure S1).

Ethical statement

All patients provided the informed written consent for collection, storage and analysis of their samples. The study was conducted in accordance with the Declaration of Helsinki and approved by the Ethics Committee of Zhongshan Hospital, Fudan University (No. B2018-193).

PNET data from International Cancer Genome Consortium (ICGC) database

Somatic variant data of 89 pNET cases from two projects (Pancreatic Cancer Endocrine Neoplasms-AU and Pancreatic Endocrine Neoplasms-IT) were downloaded from the ICGC database (https://icgc.org/). After excluding two poorly differentiated pNETs and one mixed ductal endocrine carcinoma, 86 cases were included into further analysis.

Targeted next-generation sequencing

Genomic DNA was extracted from the FFPE and fresh samples, respectively. Then, the DNA was sheared into

200–300 bp fragments by ultrasonication (Covaris, MA, USA). Sequencing libraries were prepared using Human 340-Gene Mutation Screening Kit (Euler Genomics, Beijing, China), briefly including end-repairing and A-tailing, adapter ligation, and PCR amplification. After quantity and quality assessment, the libraries hybridized with custom probes targeting all the exonic regions of 341 tumor-related genes, including those commonly mutated in pNET (for example, *MEN1*, *ATRX* and *DAXX*) (Table S1). These targeted fragments were captured using streptavidin-coated magnetic beads and then enriched by PCR. Sequencing was performed using Novaseq6000 (Illumina, San Diego, CA, USA) with 150 bp paired-end reads.

Bioinformatic analysis

FastQC (v0.11.5) was used for quality assessment of the raw sequencing reads, then the reads were aligned to the human reference genome (hg19) with Burrows-Wheeler Aligner (v0.7.13) (9). After the reads were sorted by SAMtools (v1.3.1) (10), we used Picard (v2.2.4) tools to remove the duplicate pairs. Genome Analysis ToolKit (GATK, v3.5-0) (11) was applied for local realignment around Indels and base quality recalibration. The median depths were 359× [interquartile range (IQR), 253×–432×] and 1,243× (IQR, 828×–1,613×) for normal tissues and tumors, respectively.

Germline variants were called using GATK HaplotypeCaller and annotated by ANNOVAR (v160201) (12). To identify potential pathogenic variants in genes causing pNET-associated genetic syndromes including multiple endocrine neoplasia type 1 (*MEN1*), multiple endocrine neoplasia type 4 (*CDKN1B*), Von Hippel-Lindau (*VHL*), neurofibromatosis type 1 (*NF1*), and tuberous sclerosis (*TSC1*, *TSC2*), germline variants with allele frequency >0.05 in the population databases including the 1000 Genomes Project, the Exome Aggregation Consortium, and the Exome Variant Server were excluded (13). The clinical significances of variants were interpreted with the Clinvar database (https://www.ncbi.nlm.nih.gov/clinvar/), and variants of "uncertain significance" were further predicted by algorithms including Sorting Intolerant From Tolerant (14), Polymorphism Phenotyping v2 (15), Functional Analysis through Hidden Markov Models (16), MutationTaster (17), and MutationAssessor (18). The variants predicted as "deleterious" by at least 2 algorithms without discordance were considered as "likely pathogenic".

Somatic variants were identified using GATK Mutect2 and those passing through filters were included into analysis. Variants with allele frequency <0.1 were defined as low-abundance, whereas those ≥0.1 were high-abundance (19). Mutational signatures were predicted using deconstructSigs (20) in samples with no less than 20 filtered single nucleotide variants (SNVs). Variants in coding region were selected for further analysis, and synonymous SNVs were removed when analyzing mutated genes. Putative diver genes in this cohort were detected by MutSigCV (v1.4) (21).

Somatic copy number variation (CNV) and CN-LOH were detected by Control-FREEC (v11.0) (22) using paired germline sample as a control. Genes with copy number alteration involving more than 50% of base sequence were identified.

Statistical analysis

Comparisons of continuous and categorical variables between two groups were performed with Wilcoxon rank-sum/signed-rank test and Fisher's exact test, respectively. All statistical analyses were carried out with R software (v3.6.0). A two-sided P value less than 0.05 was considered statistically significant.

Results

Patient's characteristics

Seventy-nine sequenced samples (including 29 normal tissues, 28 primary tumors, 21 liver metastases, and 1 parathyroid tumor) from 29 patients were included into analysis, and 16 of these cases had primary tumors and paired liver metastases. Among all the patients, four (13.8%) were diagnosed as MEN1, and the rest were considered as sporadic pNETs. According to the World Health Organization 2019 grading system, the vast majority (75.9%) of the cases were classified as G2. In addition, 19 patients were detected with either synchronous (n=17) or metachronous (n=2) liver metastasis. Detailed clinicopathological information was shown in Table S2.

Germline variants

A total of 82,568 germline variants (median, 2,095; IQR, 1,986–2,659) were detected from the normal tissues of pNET patients, including 58,447 SNVs (median, 1,561; IQR, 1,513–1,792) and 24,121 insertions and deletions (Indels) (median, 527; IQR, 466–804). More than 60% of the variants were located in the intergenic regions and

Table 1 Pathogenic (likely) germline variants in genes of pNET-associated genetic syndromes

Gene	Variant location	Variation type	Clinical significance	Case No.
MEN1	NM_000244.3: c.1365+1_1365+11del	Splice site	Pathogenic	25‡, 26‡
	NM_000244.3: c.1213C>T (p.Gln405Ter)	Nonsense	Pathogenic	12
	NM_000244.3: c.643_646del (p.Thr215fs)	Frameshift	Pathogenic	9‡
	NM_000244.3: c.1402G>T (p.Glu468Ter)	Nonsense	Likely pathogenic†	20‡
VHL	NM_000551.3: c.445G>A (p.Ala149Thr)	Missense	Pathogenic	16
TSC2	NM_000548.5: c.727C>T (p.Leu243Phe)	Missense	Likely pathogenic	13

†, predicted by computational algorithms; ‡, clinically diagnosed multiple endocrine neoplasia type 1. pNET, pancreatic neuroendocrine tumor.

nearly 20% were in the exonic regions. For these exonic variants, about half of the SNVs were nonsynonymous, and 60% of the indels were frameshift (Figure S2).

Four known pathogenic variants were identified in two genetic syndrome-related genes (*MEN1*, n=3; *VHL*, n=1) (*Table 1*). Three of the four clinically diagnosed MEN1 patients (cases 9, 25 and 26) were discovered with pathogenic *MEN1* variants, and the deletion in the splice site of *MEN1* (c.1365+1_1365+11del) was conformed in all the three pNET samples as well as the parathyroid tumor from a brother and sister. The remaining MEN1 patient (case 20) was detected with an unreported nonsense variant (c.1402G>T, p.Glu468Ter), which was predicted as "pathogenic" by algorithms. In addition, two patients (cases 12 and 16) without genetic syndromes were found with pathogenic germline variants in *MEN1* and *VHL*, respectively.

Somatic variants

A total of 2,471 somatic variants (median, 32; IQR, 20–57) were detected from the primary tumors (total, 1,359; median, 34; IQR, 22–58) and the liver metastases (total, 1,112; median, 31; IQR, 20–57), including 1,739 SNVs and 732 Indels, and 75.5% of these variants were low-abundance. Consistent with the previous reports, C>T (G>A) was the most common altered base type, and transition occurred much more frequently than transversion (P<0.001) (Figure S3). In the 25 samples harboring ≥20 SNVs, mutational signature analysis showed that signature 1A was detected in the 23 (92%) samples and considered as a dominant signature (weight >50%) in the 21 (84%) samples. Moreover, clustering result indicated that the liver metastatic samples harbored quite different signatures compared with the non-metastatic pNETs (Figure S4). After analyzing the variants in exonic regions, we discovered that the number of SNVs doubled than that of Indels, which was predominantly nonsynonymous, and the median exonic variants among all the samples was 26 (IQR, 14–42) (Figure S5). The identified 1,503 nonsynonymous variants affected 289 sequenced genes, and *NOTCH1* was the most frequently mutated gene, altered in the 26 (53.1%) pNET samples from 18 (62.1%) patients (*Figure 1A*). Except for *MEN1* and *ATRX*, our top 30 frequently mutated genes were rarely detected in the two cohorts from the ICGC database (*Figure 1B*).

The comparison of variants in the primary tumors from the metastatic and the non-metastatic cases showed that the metastatic patients harbored more SNVs than the non-metastatic individuals, whereas Indels distributed similarly between the two groups (*Figure 2A,2B*). More than 80% of the mutated genes detected in the non-metastatic group was also identified in the metastatic group (*Figure 2C*). By comparing the frequently altered genes (n>3), we found the higher mutation rate of *DNMT1* in the metastatic cases (52.9% *vs.* 9.1%, P=0.041) (*Figure 2D*). In addition, 16 recurrent variants involving 15 genes were identified in the primary tumors, and seven of these recurrent variants were only detected in the metastatic cases (*Figure 2E*).

On the other hand, we compared the somatic variants between the primary tumors and the paired liver metastases, and the results indicated that neither SNV nor Indel distributed differently between the two groups (*Figure 3A,3B*). Among the 278 altered genes, 55.8% were shared by the primary tumors and the metastases (*Figure 3C*). Then, we analyzed the frequently mutated genes (n>3) in the paired cases, and found the gene mutation profiles varied greatly among these individuals (*Figure 3D*). Moreover, the

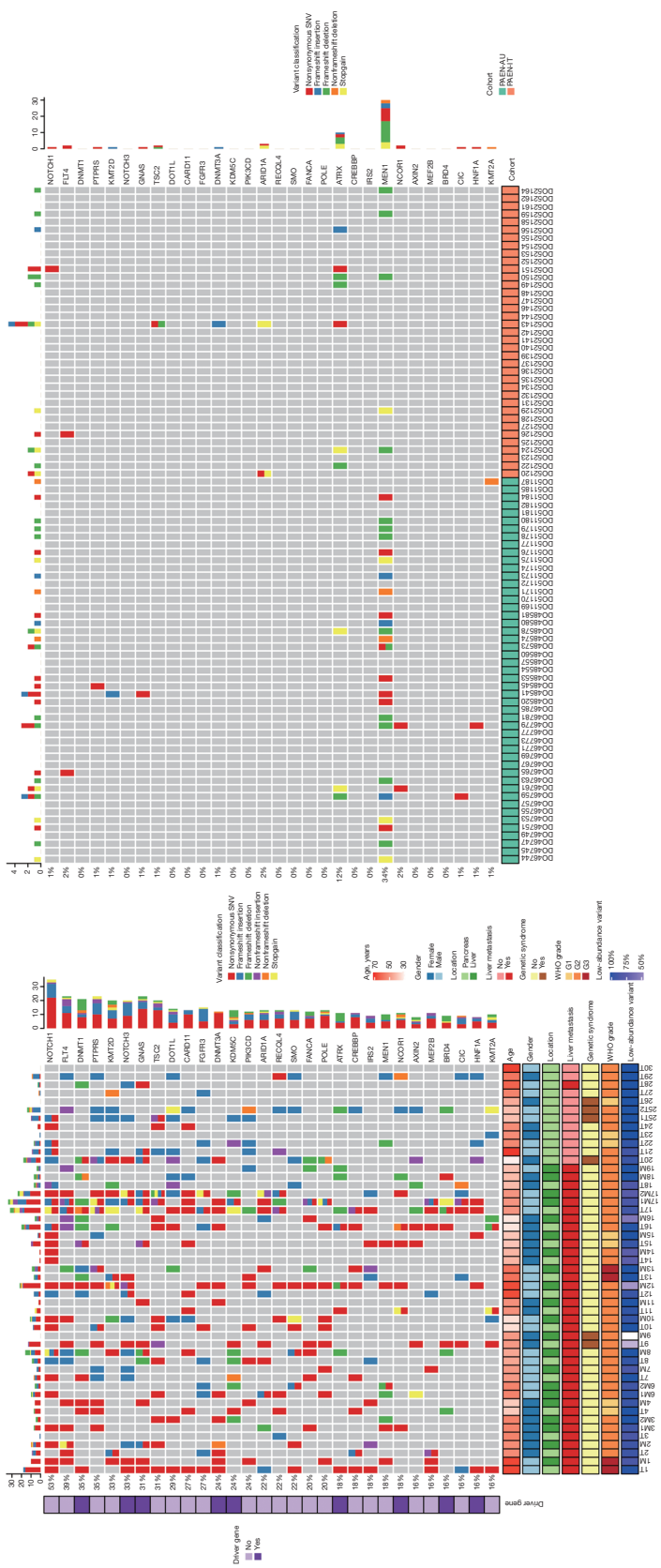

Figure 1 The top 30 frequently mutated genes in our cohort (A) and in two cohorts from the ICGC database (B). SNV, single nucleotide variant; ICGC, International Cancer Genome Consortium; PAEN-AU, pancreatic cancer endocrine neoplasms-AU; PAEN-IT, pancreatic endocrine neoplasms-IT; WHO, World Health Organization; T, primary tumor; M, liver metastasis; M1, liver metastasis 1; M2, liver metastasis 2.

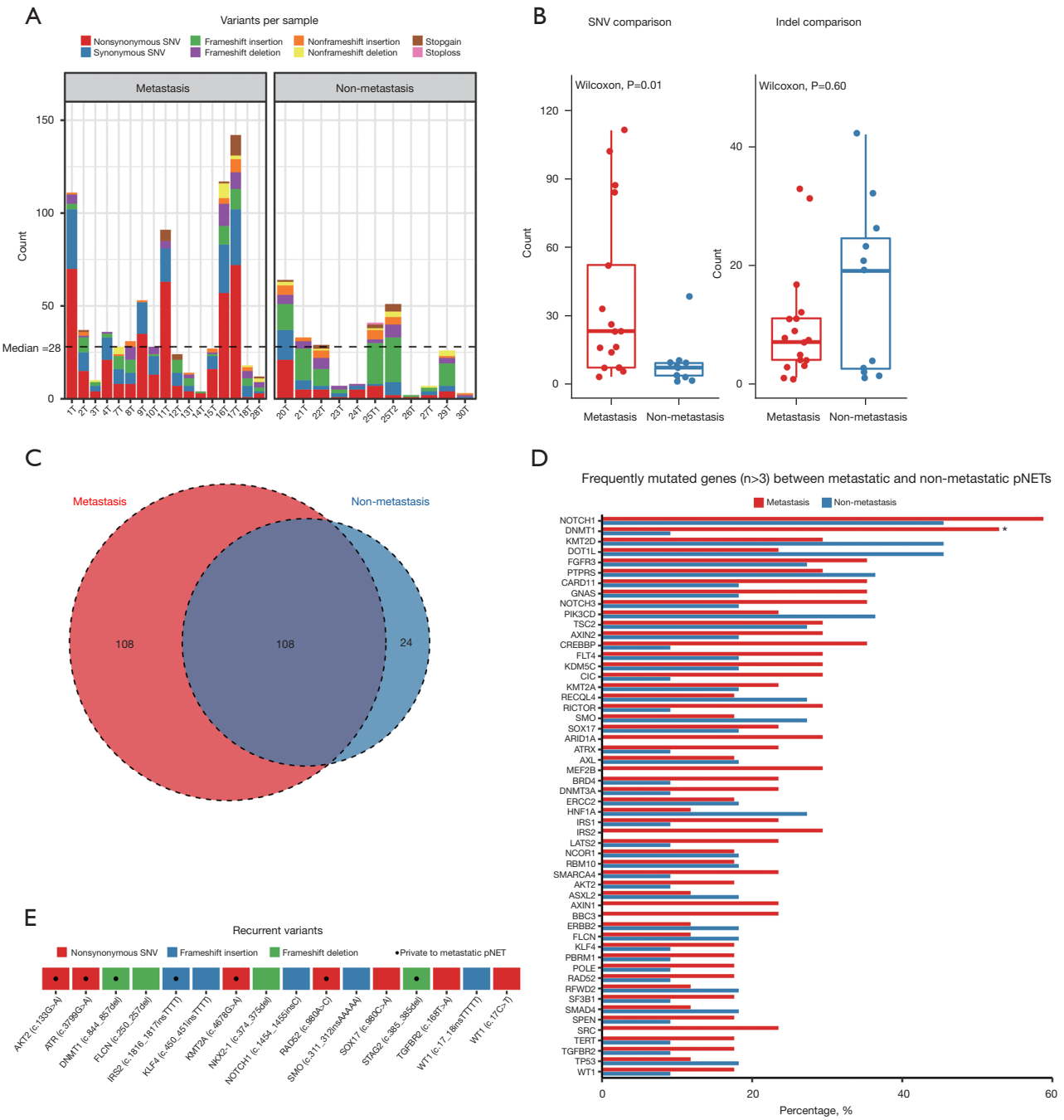

Figure 2 Somatic variants comparison in the primary pNETs grouped by liver metastasis. (A) Distribution of somatic variants; (B) comparison of somatic variants; (C) distribution of mutated genes; (D) comparison of mutated genes; (E) recurrent variants. *, P<0.05. SNV, single nucleotide variant; pNET, pancreatic neuroendocrine tumor; T, primary tumor; T1, primary tumor 1; T2, primary tumor 2.

concordance rates of mutated genes between the primary and the metastatic tumors from the same cases were quite low with a median of 10.5%. In addition, we observed that in the cases with multiple liver metastases, less than 25% of the mutated genes were shared by the metastases from the same individuals (*Figure 3E*).

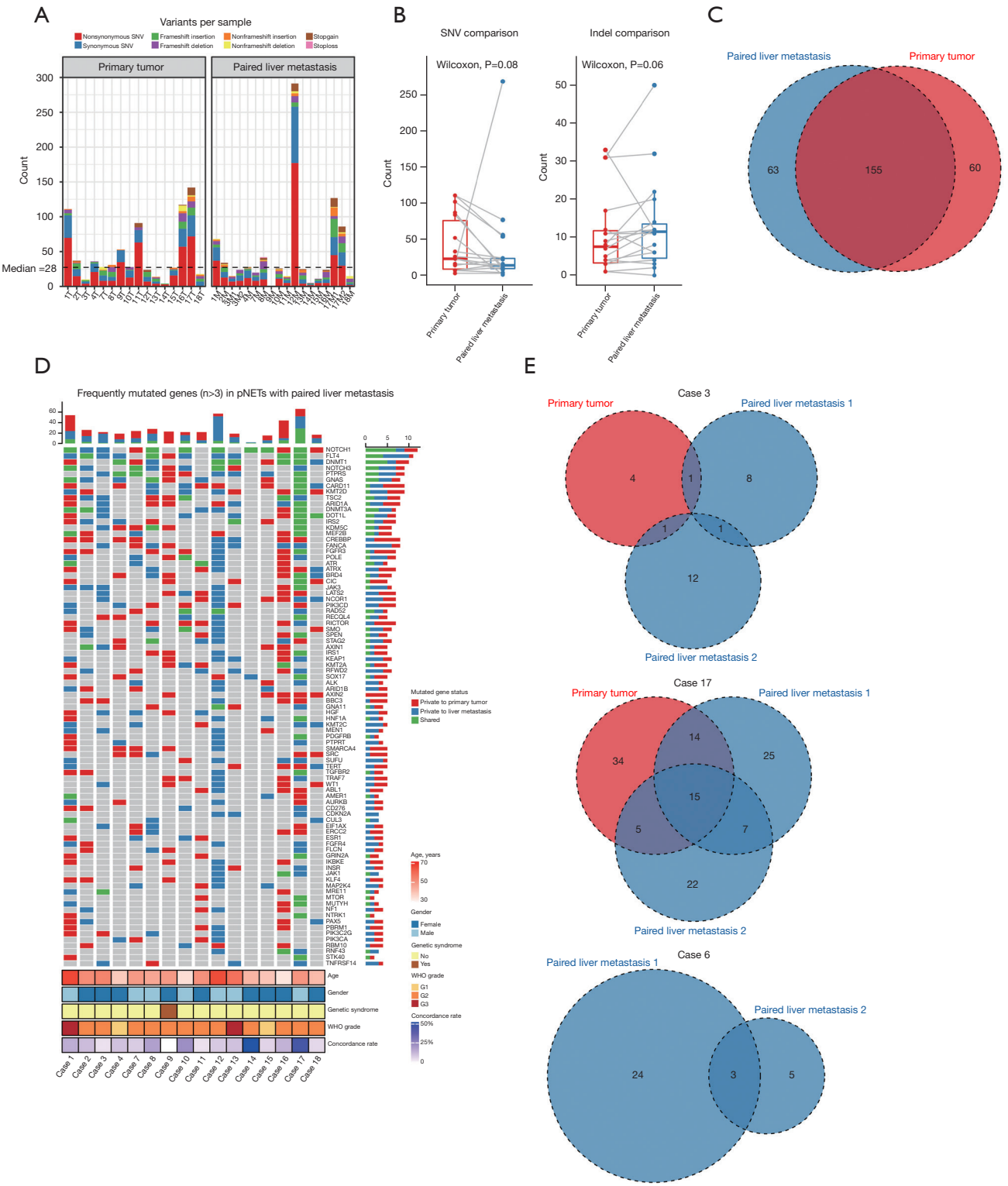

Figure 3 Somatic variants comparison in the pNET cases with paired liver metastasis. (A) Distribution of somatic variants; (B) comparison of somatic variants; (C) distribution of mutated genes; (D) profile of mutated genes in the individual cases; (E) mutated genes in the cases with multiple liver metastases. SNV, single nucleotide variant; pNET, pancreatic neuroendocrine tumor; WHO, World Health Organization; T, primary tumor; M, liver metastasis; M1, liver metastasis 1; M2, liver metastasis 2.

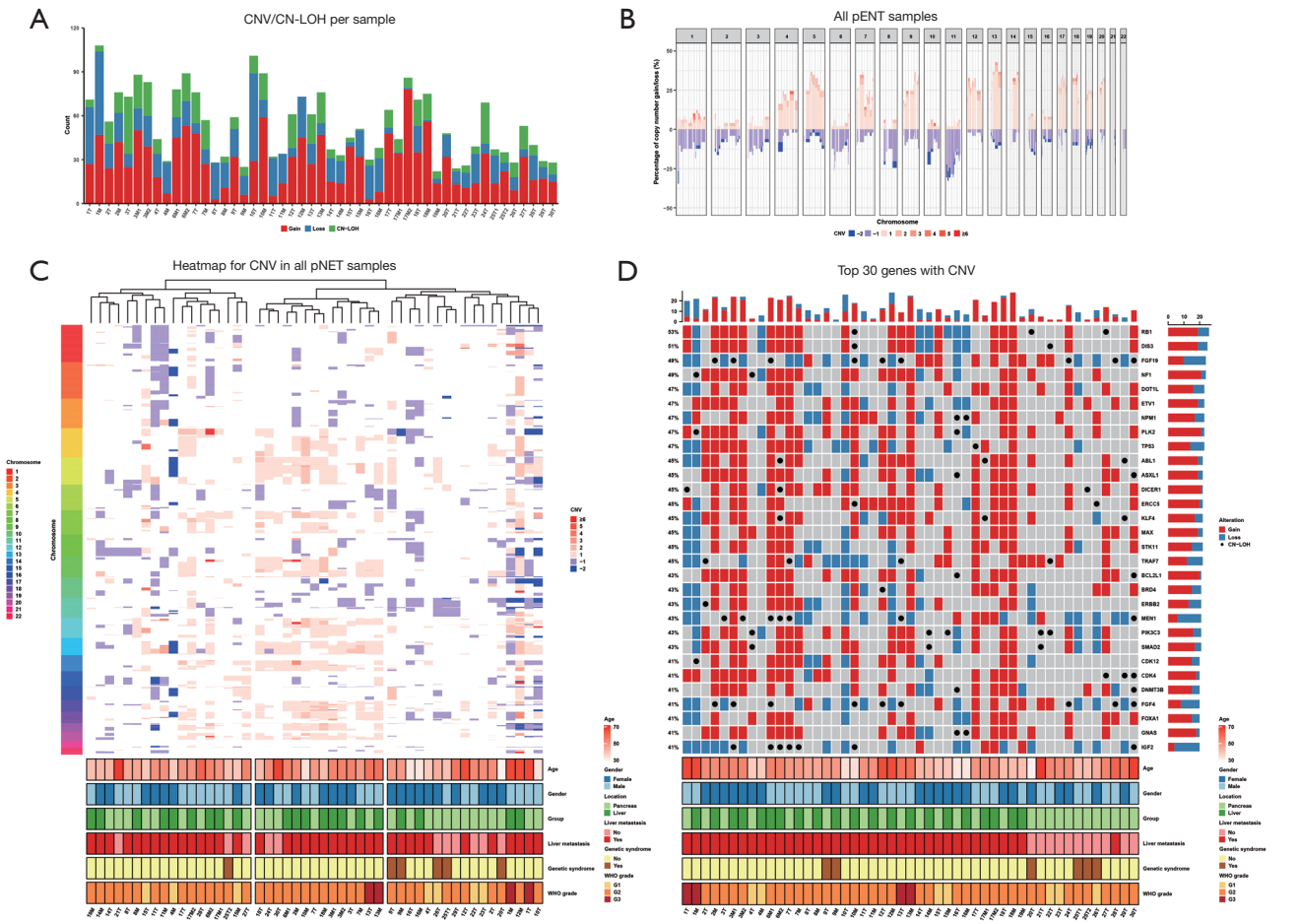

Figure 4 Somatic CNVs and CN-LOHs. (A) Distribution of somatic CNVs and CN-LOHs in every sample; (B) the proportion of somatic CNVs in every autosome; (C) heatmap of CNVs in every autosome; (D) the top 30 frequently altered genes. CNV, copy number variation; CN-LOH, copy neutral loss of heterozygosity; pNET, pancreatic neuroendocrine tumor; WHO, World Health Organization; T, primary tumor; T1, primary tumor 1; T2, primary tumor 2; M, liver metastasis; M1, liver metastasis 1; M2, liver metastasis 2.

Somatic CNV and CN-LOH

A total of 2,134 somatic CNVs (median, 37; IQR, 29–55) and 517 CN-LOHs (median, 7; IQR, 4–18) were identified in the tumor samples (*Figure 4A*). Significant copy number gains and losses were detected in chromosome 4, 5, 7, 9, 12, 13, 14, 17, 18, 19, 20 and in chromosome 11, respectively (*Figure 4B*). The CNV heatmap showed that the pNET samples could be grouped into three clusters, featured by similar number of copy number gains and losses in the left cluster, dominant copy number gains in the middle cluster, and relatively few CNVs with dominant copy number losses in the right cluster (*Figure 4C*). In addition, *RB1* was the most commonly affected gene with 19 samples detected with copy number gain and 7 with copy number loss (*Figure 4D*).

Among the primary pNETs, the metastatic cases harbored more CNVs than the non-metastatic cases (P=0.011), but no CN-LOH difference existed in the two groups. For the paired cases, neither CNV nor CN-LOH distributed differently between the primary tumors and the liver metastases (Figure S6).

Discussion

The genetic profiles of pNET are not thoroughly revealed and relatively different among previous literatures, as a consequence of its rarity and heterogeneity, and varied sequencing techniques. In this study, we conducted deep sequencing in a pNET cohort mainly consisting of liver

metastatic cases for detecting 341 tumor-related genes. Our results showed that the landscapes of mutated genes were quite different compared with those from the ICGC database. Moreover, the liver metastatic pNETs harbored more SNVs and CNVs in comparison to the non-metastatic cases. In addition, heterogeneity existed between the primary pNETs and the paired liver metastases, as well as among the different metastatic lesions from the same cases.

Approximately 10% of pNETs occur in patients with hereditary syndromes, and MEN1 is the most common genetic disease caused by germline *MEN1* inactivation, of which 40% could develop pNETs during the natural course (23). Apart from the familial and clinical criteria, genetic testing could contribute greatly to the diagnosis of MEN1 (24). In our study, three of the four MEN1 cases were detected with known pathogenic germline variants, and the remaining patient was discovered with a novel nonsense variant (c.1402G>T, p.Glu468Ter), which was predicted to be "deleterious" to the menin protein by the computational algorithms. Additionally, one patient presented with pNET as the only manifestation was found with a pathogenic germline variant. The metastatic spread of pNET is the leading cause of death for MEN1 patients, who also undergo high risks of postoperative relapse or metastasis (25). Therefore, strict surveillance is extremely important, and genetic sequencing could play a key role in confirming and discovering MEN1 candidates, particularly among those with pNET as the first manifestation.

Besides the germline alterations, somatic inactivation of *MEN1* has also been discovered in 25–44% of the sporadic cases, which plays a central role in interacting with the four well-known pathways altered in pNETs, including chromatin remodeling, telomere alteration, DNA damage repair, and mTOR signaling pathway (5,6,26). In line with the previous reports, 24.1% of our cases were detected with the somatic variants in *MEN1*, and significant copy number losses were also observed in the chromosome 11 where *MEN1* resides. Though known as a representative driver gene in pNETs, no *MEN1*-targeted therapy has been applied in the clinical practice (27). The gene replacement therapy may act as a critical treatment in the future since the vast majority of genetic alterations inactivate the corresponding encoded products in pNETs. Apart from the race difference, the low-abundance variants detected by the deep sequencing mainly resulted in the different genetic landscapes between our cohort and the ICGC database. A subset of tumor cells will develop novel genetic alterations in a time-dependent manner, which present as low-abundance variants. Vandamme *et al.* (19) demonstrated the existence of low-abundance variants in pNETs, which involved all the key pathways mentioned above, indicating the early warning effects of these variants for the high-risk candidates compared with immunohistochemistry testing. In the present study, we found *NOTCH1* was the most frequently mutated gene, altered in 62.1% of the pNET patients. As a transmembrane receptor of NOTCH signaling, NOTCH1 was previously found to be absent in pNET tissues, and enforced its expression in pNET cells could inhibit the tumor growth, indicating the suppressor role of *NOTCH1* in pNETs (28,29). Winslow *et al.* have completed a clinical trial (https://clinicaltrials.gov/, NCT01476592) regarding the activation of NOTCH1 signaling by Resveratrol in patients with low grade gastrointestinal neuroendocrine tumor, but no result has been released yet. Given the high genetic mutation frequency, activating the expression of NOTCH1 with a compound for the therapeutic intention might not be efficient or even feasible in pNETs. NOTCH3, another member of the NOTCH receptor, was also detected with a high mutation rate of 41.4%. These discoveries might imply the important value of NOTCH pathway in the genesis of pNETs, which was less explored in the previous studies.

The high proportion of liver metastatic cases in our cohort could be another explanation for the different variant profiles. Among the primary lesions, metastatic cases harbored more SNVs and CNVs than the non-metastatic counterparts, indicating the increased genomic instability in the metastatic group. Similar results could be found in the previous work regarding small pNETs that the group with high-risk of liver metastasis was featured with more somatic mutations and recurrent chromosomal gains (8). Thus, the high number of SNVs and CNVs could be related to the frequent development of metastasis, which may become potential metastatic biomarkers for the pNET patients. All mutated genes but *DNMT1* distributed similarly between metastatic and non-metastatic pNETs. DNMT1, a member of the DNA methyltransferase family, is mainly required for maintaining the methylation status following DNA replication (30). The mutation rate of *DNMT1* was significantly high in the metastatic cases (52.9% *vs.* 9.1%, P=0.016), and a recurrent mutation (c.844_857del, p.Asp282fs) was also observed in this group. Previously, Roy *et al.* (7) also reported that 10% of the pNET distant metastases were detected with the alterations in *DNMT1* by the whole-exome sequencing. Though no statistical difference was reached, DNMT3A, a *de-novo*

methyltransferase, seemed to mutate more frequently in the metastatic pNETs (23.5% *vs.* 9.1%), adding the potential role of epigenetic modification in participating in the metastasis process of pNETs.

Characterized by the heterogeneity, pNETs show various biological behaviors and clinical manifestations, which might reflect the heterogeneous alterations in the genomes. Among the patients with paired liver metastases, the mutation rates of sequenced genes varied greatly. More importantly, the primary and the metastatic lesions from the same patient shared quite limited mutated genes, which was also observed in the different metastatic lesions from the same primary tumor. Currently, chemotherapy and targeted therapy are the major treatments for the metastatic patients (31). Given the genomic heterogeneity, the clinically routine biopsy of the metastatic lesion, which is a relatively safe procedure compared with the pancreatic puncture, may not be sufficient enough to evaluate individual's genetic feature to guide the subsequent treatments. Worse still, the low-abundance variants derived from a fraction of tumor cells, called subclones, also challenge the power of biopsy to thoroughly reveal the whole genetic profile in a single pNET lesion. It is urgent to seek effective ways to fully assess the genetic status for every pNET patient in the current area of precision medicine.

Several limitations regarding our study should be mentioned. First, the sample size is relatively small, and we could not powerfully analyze the clinical significances of these genetic alterations here. Second, the low-abundance variants could not be validated owing to the current techniques. In addition, no data with regards to transcription, translation or biological function could be provided at present. Anyway, we hope the current research could deepen the understanding for the genetic features of this rare tumor, particularly for the metastatic pNETs.

In conclusion, through the 341 tumor-related genes targeted deep sequencing, we identified quite a few low-abundance variants in the pNETs, implying the intratumor heterogeneity. Moreover, primary and metastatic tumors from the same individual shared limited common gene mutations, challenging the genetic results from a single lesion in guiding the systemic treatment. In addition, different metastatic pNET patients harbored greatly varied genetic profiles, highlighting the importance of precision medicine in such heterogeneous entities. Multi-omics and functional studies are needed to comprehensively reveal the subsequent alterations following genomic variants, and to clarify the corresponding effects on the biological processes for pNETs in the future.

Acknowledgments

We would like to thank Dr. Suming Huang for her help with sample collection and Prof. Jingjing Li for her advice of manuscript revision.
Funding: This work was supported by the Science and Technology Commission of Shanghai Municipality (No.19140901700).

Footnote

Reporting Checklist: The authors have completed the STREGA reporting checklist. Available at https://hbsn.amegroups.com/article/view/10.21037/hbsn-21-413/rc

Data Sharing Statement: Available at https://hbsn.amegroups.com/article/view/10.21037/hbsn-21-413/dss

Conflicts of Interest: All authors have completed the ICMJE uniform disclosure form (available at https://hbsn.amegroups.com/article/view/10.21037/hbsn-21-413/coif). The authors have no conflicts of interest to declare.

Ethical Statement: The authors are accountable for all aspects of the work in ensuring that questions related to the accuracy or integrity of any part of the work are appropriately investigated and resolved. All patients provided the informed written consent for collection, storage and analysis of their samples. The study was conducted in accordance with the Declaration of Helsinki and was approved by the Ethics Committee of Zhongshan Hospital, Fudan University (No. B2018-193).

References

1. Gordon-Dseagu VL, Devesa SS, Goggins M, et al. Pancreatic cancer incidence trends: evidence from the Surveillance, Epidemiology and End Results (SEER) population-based data. Int J Epidemiol 2018;47:427-39.
2. Luo G, Fan Z, Gong Y, et al. Characteristics and Outcomes of Pancreatic Cancer by Histological Subtypes. Pancreas 2019;48:817-22.
3. Dasari A, Shen C, Halperin D, et al. Trends in the Incidence, Prevalence, and Survival Outcomes in Patients With Neuroendocrine Tumors in the United States. JAMA Oncol 2017;3:1335-42.
4. Yao JC, Eisner MP, Leary C, et al. Population-based study of islet cell carcinoma. Ann Surg Oncol 2007;14:3492-500.
5. Jiao Y, Shi C, Edil BH, et al. DAXX/ATRX, MEN1, and mTOR pathway genes are frequently altered in pancreatic neuroendocrine tumors. Science 2011;331:1199-203.
6. Scarpa A, Chang DK, Nones K, et al. Whole-genome landscape of pancreatic neuroendocrine tumours. Nature 2017;543:65-71.
7. Roy S, LaFramboise WA, Liu TC, et al. Loss of Chromatin-Remodeling Proteins and/or CDKN2A Associates With Metastasis of Pancreatic Neuroendocrine Tumors and Reduced Patient Survival Times. Gastroenterology 2018;154:2060-3.e8.
8. Pea A, Yu J, Marchionni L, et al. Genetic Analysis of Small Well-differentiated Pancreatic Neuroendocrine Tumors Identifies Subgroups With Differing Risks of Liver Metastases. Ann Surg 2020;271:566-73.
9. Li H, Durbin R. Fast and accurate long-read alignment with Burrows-Wheeler transform. Bioinformatics 2010;26:589-95.
10. Li H, Handsaker B, Wysoker A, et al. The Sequence Alignment/Map format and SAMtools. Bioinformatics 2009;25:2078-9.
11. McKenna A, Hanna M, Banks E, et al. The Genome Analysis Toolkit: a MapReduce framework for analyzing next-generation DNA sequencing data. Genome Res 2010;20:1297-303.
12. Wang K, Li M, Hakonarson H. ANNOVAR: functional annotation of genetic variants from high-throughput sequencing data. Nucleic Acids Res 2010;38:e164.
13. Richards S, Aziz N, Bale S, et al. Standards and guidelines for the interpretation of sequence variants: a joint consensus recommendation of the American College of Medical Genetics and Genomics and the Association for Molecular Pathology. Genet Med 2015;17:405-24.
14. Kumar P, Henikoff S, Ng PC. Predicting the effects of coding non-synonymous variants on protein function using the SIFT algorithm. Nat Protoc 2009;4:1073-81.
15. Adzhubei IA, Schmidt S, Peshkin L, et al. A method and server for predicting damaging missense mutations. Nat Methods 2010;7:248-9.
16. Shihab HA, Gough J, Cooper DN, et al. Predicting the functional, molecular, and phenotypic consequences of amino acid substitutions using hidden Markov models. Hum Mutat 2013;34:57-65.
17. Schwarz JM, Rödelsperger C, Schuelke M, et al. MutationTaster evaluates disease-causing potential of sequence alterations. Nat Methods 2010;7:575-6.
18. Reva B, Antipin Y, Sander C. Predicting the functional impact of protein mutations: application to cancer genomics. Nucleic Acids Res 2011;39:e118.
19. Vandamme T, Beyens M, Boons G, et al. Hotspot DAXX, PTCH2 and CYFIP2 mutations in pancreatic neuroendocrine neoplasms. Endocr Relat Cancer 2019;26:1-12.
20. Rosenthal R, McGranahan N, Herrero J, et al. DeconstructSigs: delineating mutational processes in single tumors distinguishes DNA repair deficiencies and patterns of carcinoma evolution. Genome Biol 2016;17:31.
21. Lawrence MS, Stojanov P, Polak P, et al. Mutational heterogeneity in cancer and the search for new cancer-associated genes. Nature 2013;499:214-8.
22. Boeva V, Popova T, Bleakley K, et al. Control-FREEC: a tool for assessing copy number and allelic content using next-generation sequencing data. Bioinformatics 2012;28:423-5.
23. Thakker RV. Multiple endocrine neoplasia type 1 (MEN1) and type 4 (MEN4). Mol Cell Endocrinol 2014;386:2-15.
24. Thakker RV, Newey PJ, Walls GV, et al. Clinical practice guidelines for multiple endocrine neoplasia type 1 (MEN1). J Clin Endocrinol Metab 2012;97:2990-3011.
25. Sonoda A, Yamashita YI, Kondo T, et al. Clinicopathological features and menin expression of pancreatic neuroendocrine neoplasm associated with multiple endocrine neoplasia type 1. J Hepatobiliary Pancreat Sci 2020;27:984-91.
26. Mafficini A, Scarpa A. Genetics and Epigenetics of Gastroenteropancreatic Neuroendocrine Neoplasms. Endocr Rev 2019;40:506-36.
27. Stevenson M, Lines KE, Thakker RV. Molecular Genetic Studies of Pancreatic Neuroendocrine Tumors: New Therapeutic Approaches. Endocrinol Metab Clin North Am 2018;47:525-48.

28. Wang H, Chen Y, Fernandez-Del Castillo C, et al. Heterogeneity in signaling pathways of gastroenteropancreatic neuroendocrine tumors: a critical look at notch signaling pathway. Mod Pathol 2013;26:139-47.
29. Kunnimalaiyaan M, Traeger K, Chen H. Conservation of the Notch1 signaling pathway in gastrointestinal carcinoid cells. Am J Physiol Gastrointest Liver Physiol 2005;289:G636-42.
30. Zhang J, Yang C, Wu C, et al. DNA Methyltransferases in Cancer: Biology, Paradox, Aberrations, and Targeted Therapy. Cancers (Basel) 2020;12:2123.
31. Pavel M, O'Toole D, Costa F, et al. ENETS Consensus Guidelines Update for the Management of Distant Metastatic Disease of Intestinal, Pancreatic, Bronchial Neuroendocrine Neoplasms (NEN) and NEN of Unknown Primary Site. Neuroendocrinology 2016;103:172-85.

Cite this article as: Zhou W, Han X, Ji Y, Wang D, Xie D, Qiu Z, Lou W. Targeted deep sequencing reveals the genetic heterogeneity in well-differentiated pancreatic neuroendocrine tumors with liver metastasis. HepatoBiliary Surg Nutr 2023;12(3):302-313. doi: 10.21037/hbsn-21-413

Table S1 Gene panel

341 tumor-related genes								
ABL1	*CASP8*	*E2F3*	*FOXA1*	*KDM5A*	*MYOD1*	*PMAIP1*	*SDHA*	*TP63*
AKT1	*CBFB*	*EED*	*FOXL2*	*KDM5C*	*NBN*	*PMS1*	*SDHAF2*	*TRAF7*
AKT2	*CBL*	*EGFL7*	*FOXP1*	*KDM6A*	*NCOR1*	*PMS2*	*SDHB*	*TSC1*
AKT3	*CCND1*	*EGFR*	*FUBP1*	*KDR*	*NF1*	*PNRC1*	*SDHC*	*TSC2*
ALK	*CCND2*	*EIF1AX*	*GATA1*	*KEAP1*	*NF2*	*POLE*	*SDHD*	*TSHR*
ALOX12B	*CCND3*	*EP300*	*GATA2*	*KIT*	*NFE2L2*	*PPP2R1A*	*SETD2*	*U2AF1*
APC	*CCNE1*	*EPCAM*	*GATA3*	*KLF4*	*NKX2-1*	*PRDM1*	*SF3B1*	*VHL*
AR	*CD274*	*EPHA3*	*GNA11*	*KRAS*	*NKX3-1*	*PRKAR1A*	*SH2D1A*	*VTCN1*
ARAF	*CD276*	*EPHA5*	*GNAQ*	*LATS1*	*NOTCH1*	*PTCH1*	*SHQ1*	*WT1*
ARID1A	*CD79B*	*EPHB1*	*GNAS*	*LATS2*	*NOTCH2*	*PTEN*	*SMAD2*	*XIAP*
ARID1B	*CDC73*	*ERBB2*	*GREM1*	*LMO1*	*NOTCH3*	*PTPN11*	*SMAD3*	*XPO1*
ARID2	*CDH1*	*ERBB3*	*GRIN2A*	*MAP2K1*	*NOTCH4*	*PTPRD*	*SMAD4*	*YAP1*
ARID5B	*CDK12*	*ERBB4*	*GSK3B*	*MAP2K2*	*NPM1*	*PTPRS*	*SMARCA4*	*YES1*
ASXL1	*CDK4*	*ERCC2*	*H3F3C*	*MAP2K4*	*NRAS*	*PTPRT*	*SMARCB1*	
ASXL2	*CDK6*	*ERCC3*	*HGF*	*MAP3K1*	*NSD1*	*RAC1*	*SMARCD1*	
ATM	*CDK8*	*ERCC4*	*HIST1H1C*	*MAP3K13*	*NTRK1*	*RAD50*	*SMO*	
ATR	*CDKN1A*	*ERCC5*	*HIST1H2BD*	*MAPK1*	*NTRK2*	*RAD51*	*SOCS1*	
ATRX	*CDKN1B*	*ERG*	*HIST1H3B*	*MAX*	*NTRK3*	*RAD51B*	*SOX17*	
AURKA	*CDKN2A*	*ESR1*	*HNF1A*	*MCL1*	*PAK1*	*RAD51C*	*SOX2*	
AURKB	*CDKN2B*	*ETV1*	*HRAS*	*MDC1*	*PAK7*	*RAD51D*	*SOX9*	
AXIN1	*CDKN2C*	*ETV6*	*ICOSLG*	*MDM2*	*PALB2*	*RAD52*	*SPEN*	
AXIN2	*CHEK1*	*EZH2*	*IDH1*	*MDM4*	*PARK2*	*RAD54L*	*SPOP*	
AXL	*CHEK2*	*FAM123B*	*IDH2*	*MED12*	*PARP1*	*RAF1*	*SRC*	
B2M	*CIC*	*FAM175A*	*IFNGR1*	*MEF2B*	*PAX5*	*RARA*	*STAG2*	
BAP1	*CREBBP*	*FAM46C*	*IGF1*	*MEN1*	*PBRM1*	*RASA1*	*STK11*	
BARD1	*CRKL*	*FANCA*	*IGF1R*	*MET*	*PDCD1*	*RB1*	*STK40*	
BBC3	*CRLF2*	*FANCC*	*IGF2*	*MITF*	*PDGFRA*	*RBM10*	*SUFU*	
BCL2	*CSF1R*	*FAT1*	*IKBKE*	*MLH1*	*PDGFRB*	*RECQL4*	*SUZ12*	
BCL2L1	*CTCF*	*FBXW7*	*IKZF1*	*MLL*	*PDPK1*	*REL*	*SYK*	
BCL2L11	*CTLA4*	*FGF19*	*IL10*	*MLL2*	*PHOX2B*	*RET*	*TBX3*	
BCL6	*CTNNB1*	*FGF3*	*IL7R*	*MLL3*	*PIK3C2G*	*RFWD2*	*TERT*	
BCOR	*CUL3*	*FGF4*	*INPP4A*	*MPL*	*PIK3C3*	*RHOA*	*TET1*	
BLM	*DAXX*	*FGFR1*	*INPP4B*	*MRE11A*	*PIK3CA*	*RICTOR*	*TET2*	
BMPR1A	*DCUN1D1*	*FGFR2*	*INSR*	*MSH2*	*PIK3CB*	*RIT1*	*TGFBR1*	
BRAF	*DDR2*	*FGFR3*	*IRF4*	*MSH6*	*PIK3CD*	*RNF43*	*TGFBR2*	
BRCA1	*DICER1*	*FGFR4*	*IRS1*	*MTOR*	*PIK3CG*	*ROS1*	*TMEM127*	
BRCA2	*DIS3*	*FH*	*IRS2*	*MUTYH*	*PIK3R1*	*RPS6KA4*	*TMPRSS2*	
BRD4	*DNMT1*	*FLCN*	*JAK1*	*MYC*	*PIK3R2*	*RPS6KB2*	*TNFAIP3*	
BRIP1	*DNMT3A*	*FLT1*	*JAK2*	*MYCL1*	*PIK3R3*	*RPTOR*	*TNFRSF14*	
BTK	*DNMT3B*	*FLT3*	*JAK3*	*MYCN*	*PIM1*	*RUNX1*	*TOP1*	
CARD11	*DOT1L*	*FLT4*	*JUN*	*MYD88*	*PLK2*	*RYBP*	*TP53*	

https://dx.doi.org/10.21037/hbsn-21-413

Table S2 Clinicopathological characteristics of pNET patients

Parameters	N=29
Age at pNET resection, years, median [IQR]	51 [42–54]
Sex, n (%)	
Male	15 (51.7)
Female	14 (48.3)
Genetic syndrome, n (%)	
MEN1	4 (13.8)
Sporadic	25 (86.2)
Primary tumor	
Location, n (%)	
Head/neck	7 (24.1)
Body/tail	21 (72.4)
Both	1 (3.4)
Operation, n (%)	
Pancreaticoduodenectomy	3 (10.3)
Distal pancreatectomy	20 (69.0)
Total pancreatectomy	1 (3.4)
Enucleation	3 (10.3)
Segmental resection	1 (3.4)
No resection	1 (3.4)
Number, n (%)	
Solitary	26 (89.7)
Multiple	3 (10.3)
Diameter of the largest lesion, cm, median [IQR]	3.4 [2.0–5.0]
Necrosis, n (%)	
Yes	3 (10.3)
No	25 (86.2)
NA	1 (3.4)
Margin status, n (%)	
Negative	27 (93.1)
Positive	1 (3.4)
NA	1 (3.4)
Perineural invasion, n (%)	
Yes	11 (37.9)
No	17 (58.6)
NA	1 (3.4)
Microvascular invasion, n (%)	
Yes	7 (24.1)
No	21 (72.4)
NA	1 (3.4)
2019 WHO grade, n (%)	
G1	5 (17.2)
G2	22 (75.9)
G3	2 (6.9)
Liver metastasis	n=19
Number, n (%)	
Solitary	5 (26.3)
Multiple	14 (73.7)
Synchronous metastasis, n (%)	
Yes	17 (89.5)
No	2 (10.5)
Diameter of the largest lesion, cm, median [IQR]	2.5 [1.6–3.0]

pNET, pancreatic neuroendocrine tumor; MEN1, multiple endocrine neoplasia type 1; WHO, World Health Organization; IQR, interquartile range; NA, not available.

https://dx.doi.org/10.21037/hbsn-21-413

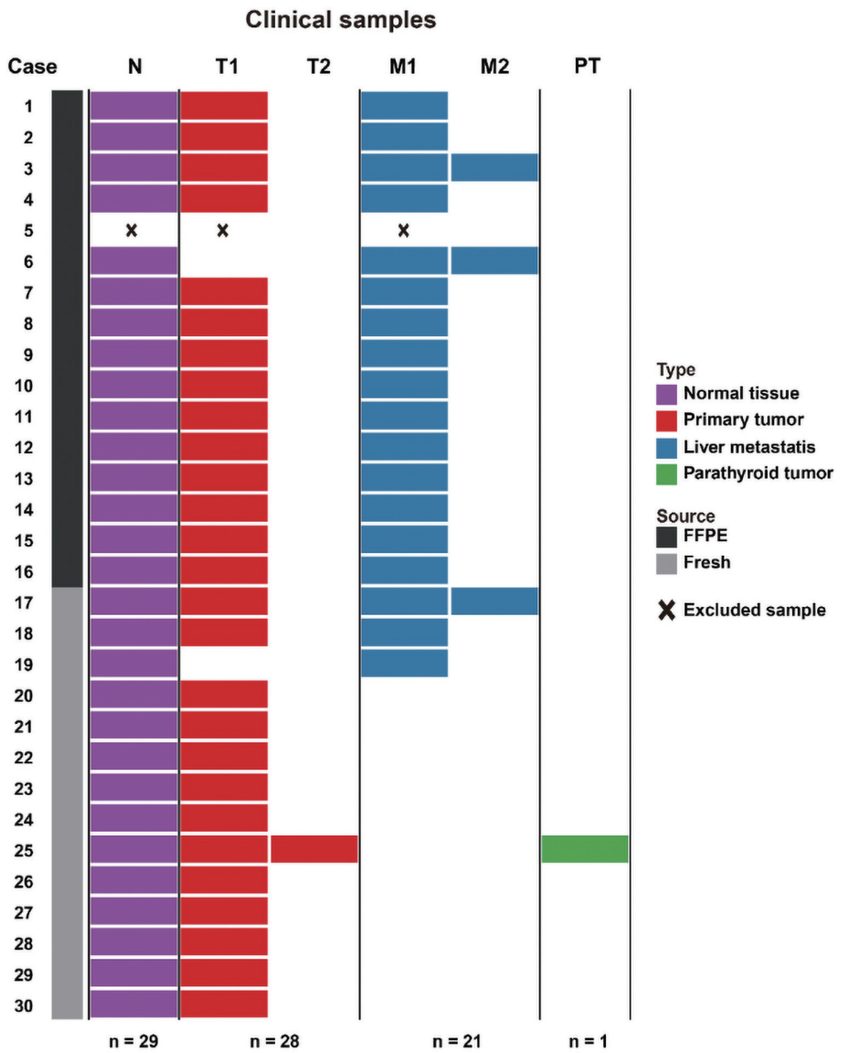

Figure S1 Detailed information of the collected samples for sequencing. N, normal tissue; T, primary tumor; T1, primary tumor 1; T2, primary tumor 2; M, liver metastasis; M1, liver metastasis 1; M2, liver metastasis 2; PT, parathyroid tumor; FFPE, formalin-fixed, paraffin-embedded.

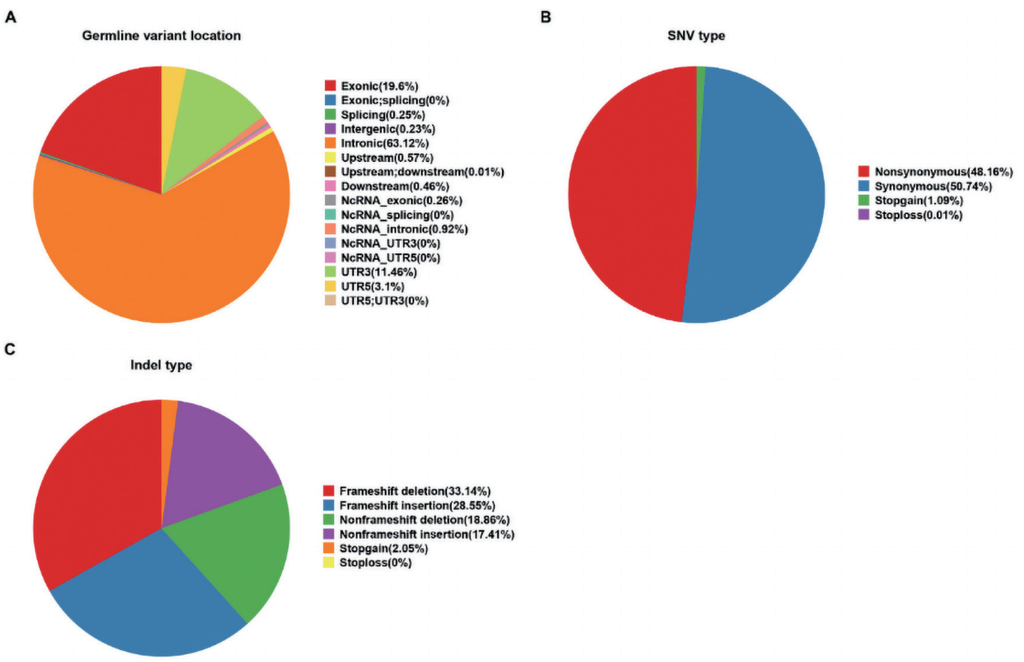

Figure S2 Germline variant classification. The constituent ratios of variant location (A), exonic SNV function (B), and Indel function (C). SNV, single nucleotide variant; Indel, insertion and deletion; NcRNA, non-coding RNA; UTR, untranslated region.

https://dx.doi.org/10.21037/hbsn-21-413

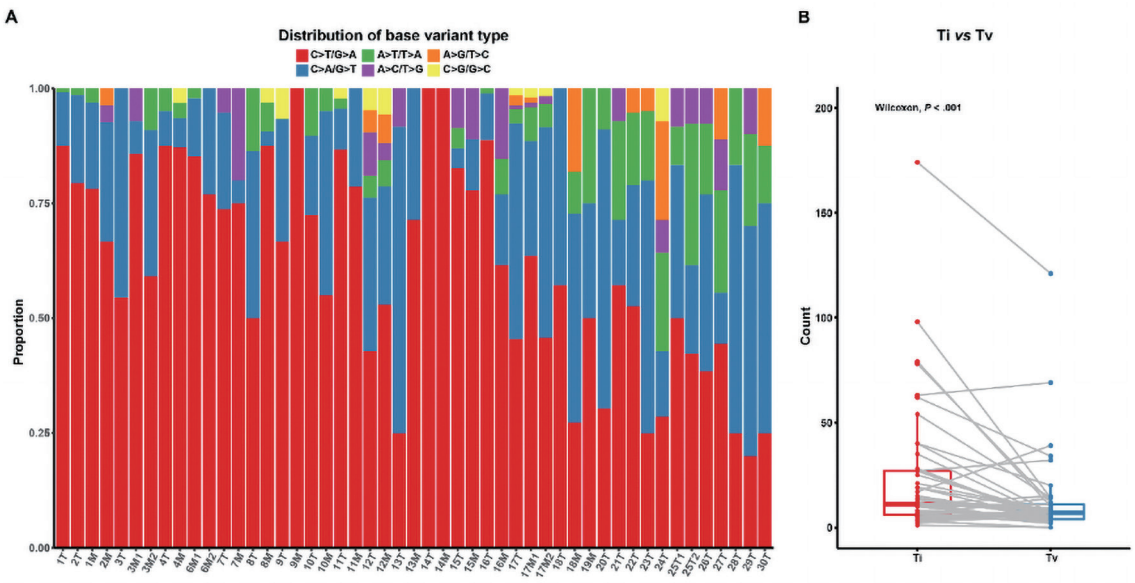

Figure S3 Somatic base alteration type. (A) Distribution of somatic base alteration type in every sample; (B) comparison of transition and transversion. Ti, transition; Tv, transversion; T, primary tumor; T1, primary tumor 1; T2, primary tumor 2; M, liver metastasis; M1, liver metastasis 1; M2, liver metastasis 2.

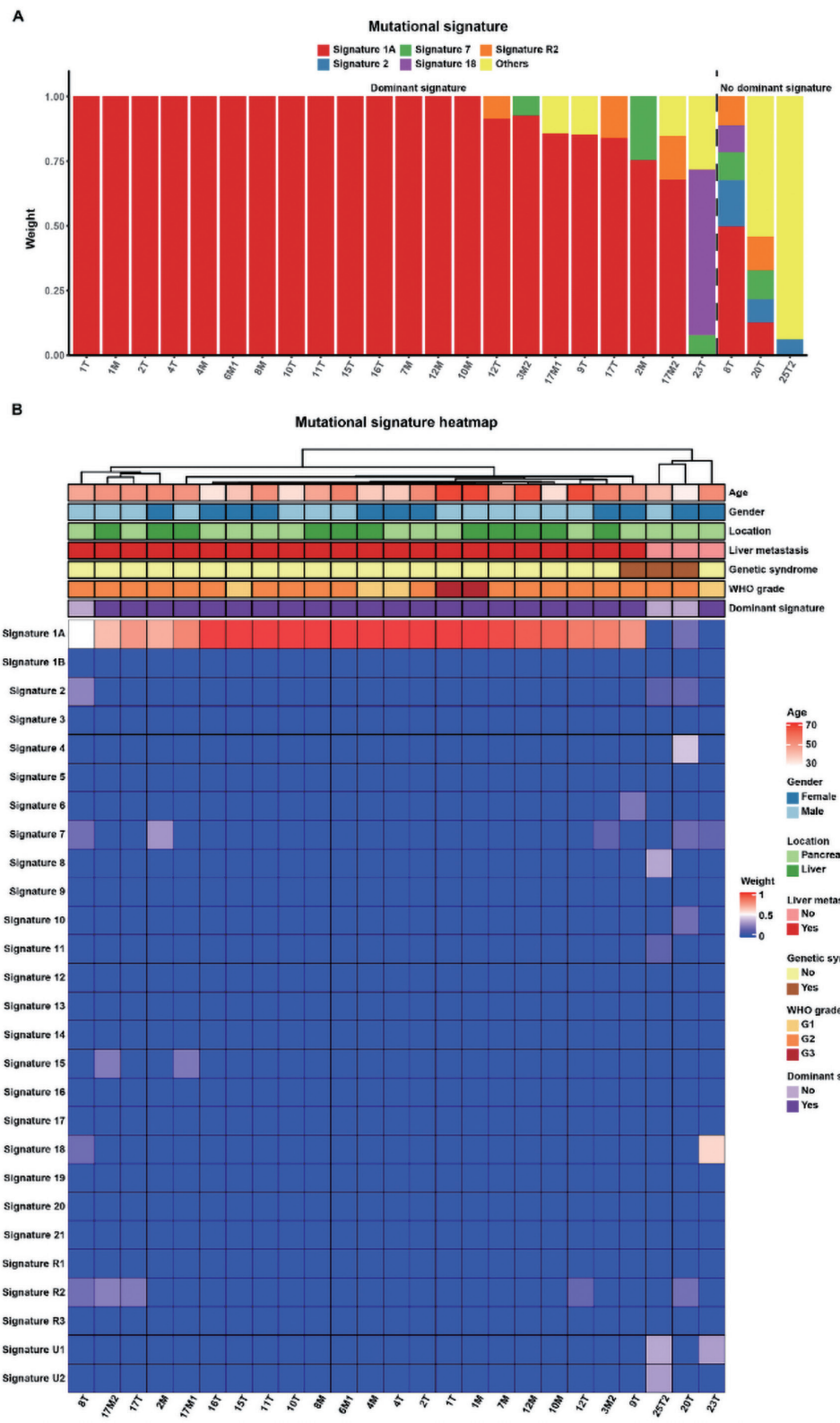

Figure S4 Mutational signatures. (A) Distribution of mutational signatures in the samples harboring ≥20 SNVs; (B) clustering analysis. SNVs, single nucleotide variants; WHO, World Health Organization; T, primary tumor; T1, primary tumor 1; T2, primary tumor 2; M, liver metastasis; M1, liver metastasis 1; M2, liver metastasis 2.

https://dx.doi.org/10.21037/hbsn-21-413

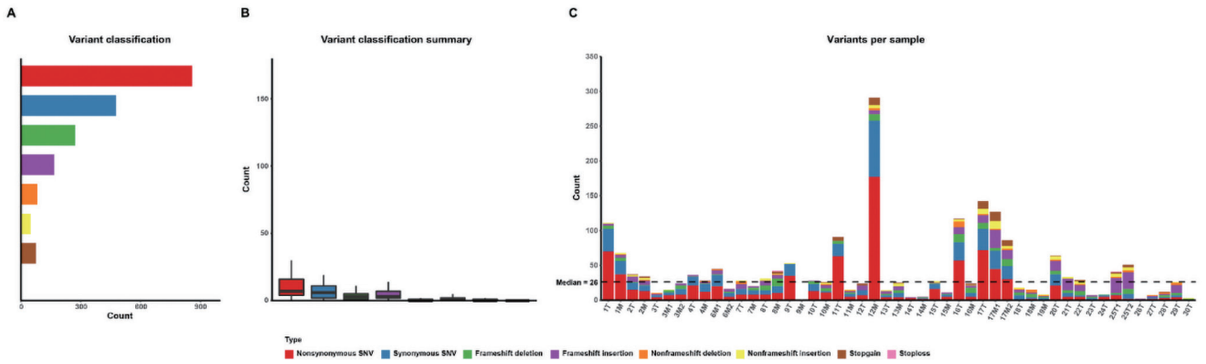

Figure S5 Classification (A,B) and distribution (C) of somatic variants in the exonic regions. SNV, single nucleotide variant; Indel, insertion and deletion; T, primary tumor; T1, primary tumor 1; T2, primary tumor 2; M, liver metastasis; M1, liver metastasis 1; M2, liver metastasis 2.

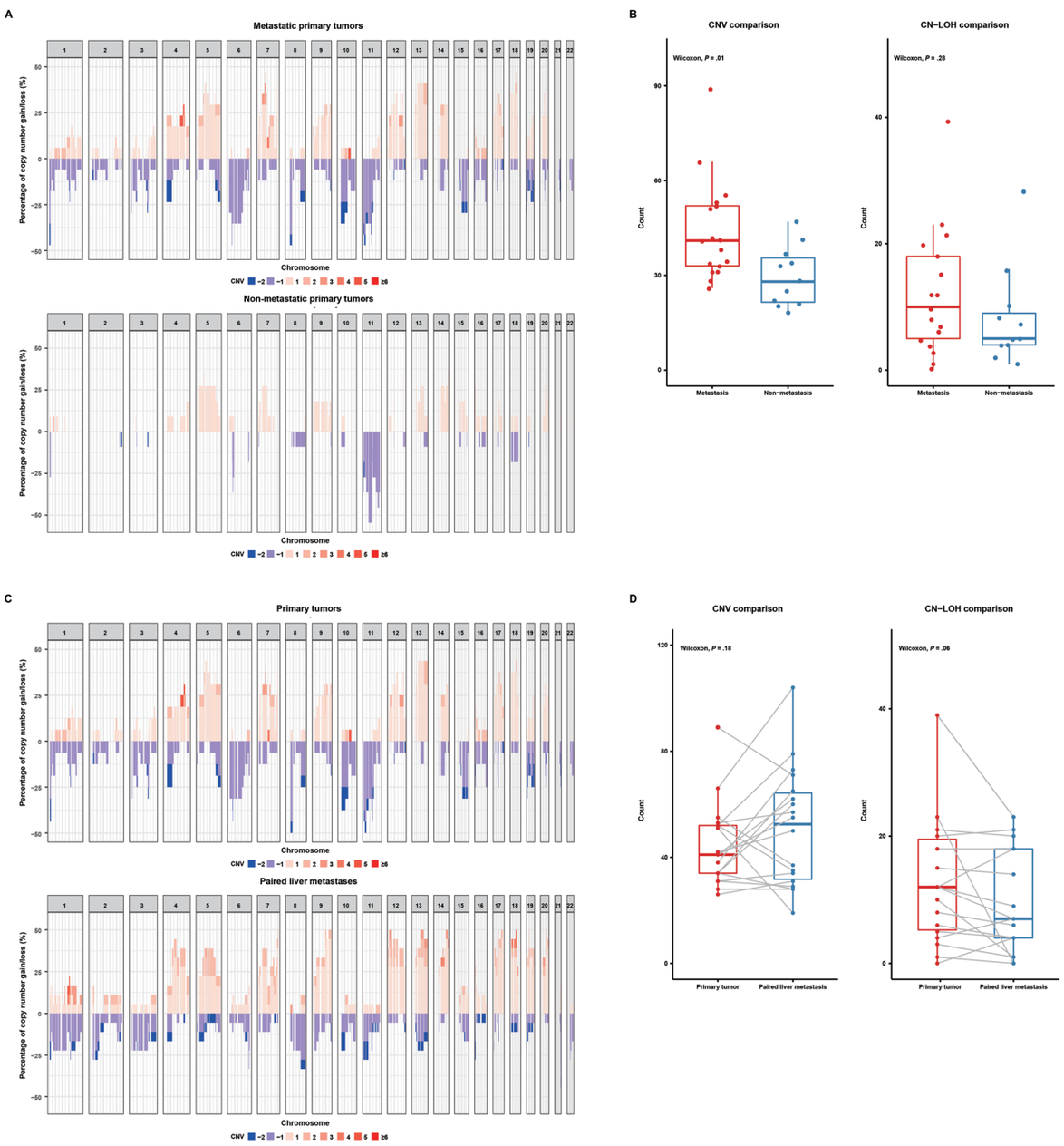

Figure S6 Distribution and comparison of somatic CNVs and CN-LOHs. (A) The proportion of CNVs in the primary pNETs grouped by liver metastasis; (B) comparison of CNVs and CN-LOHs in the primary pNETs; (C) the proportion of CNVs in the paired metastatic pNET cases; (D) comparison of CNVs and CN-LOHs in the paired metastatic pNET cases. pNET, pancreatic neuroendocrine tumor; CNV, copy number variation; CN-LOH, copy neutral loss of heterozygosity.

https://dx.doi.org/10.21037/hbsn-21-413